

## Supporting Information

### Functionalized Sc<sub>2</sub>N as Ohmic contacted electrodes for Monolayer

#### PtSe<sub>2</sub>: An *ab initio* Study

Hong Li<sup>1,\*</sup>, Jiahui Li<sup>1</sup>, Chaoyang Fan<sup>1</sup>, Fengbin Liu<sup>1</sup>, Shuai Sun<sup>1</sup>, and Jing Lu<sup>2,3,4\*</sup>

<sup>1</sup> College of Mechanical and Material Engineering, North China University of Technology,  
Beijing 100144, P. R. China

<sup>2</sup> State Key Laboratory of Mesoscopic Physics and Department of Physics, Peking University,  
Beijing 100871, P. R. China

<sup>3</sup> Collaborative Innovation Center of Quantum Matter, Beijing 100871, P. R. China

<sup>4</sup> Peking University Yangtze Delta Institute of Optoelectronics, Nantong 226000, P. R. China

\*Corresponding author: jinglu@pku.edu.cn; lihong@ncut.edu.cn

**Table S1.** The lattice mismatch, interlayer distance ( $d$ ), binding energy ( $E_b$ ), band gap ( $E_g$ ), vertical Schottky barriers ( $\Phi_n^\perp/\Phi_p^\perp$ ), and lateral Schottky barriers ( $\Phi_n^{\parallel\parallel}/\Phi_p^{\parallel\parallel}$ ) of the PtSe<sub>2</sub>/Sc<sub>2</sub>N and PtSe<sub>2</sub>/Sc<sub>2</sub>NX<sub>2</sub> (X = F, O, and OH) vertical heterojunctions with supercells of  $(\sqrt{3} \times \sqrt{3})/(2 \times 2)$ .

	mismatch	$d$	$E_b$	$E_g$	$\Phi_n^\perp/\Phi_p^\perp$	$\Phi_n^{\parallel\parallel}/\Phi_p^{\parallel\parallel}$
		(Å)	(meV/Å <sup>2</sup> )	(eV)	(eV)	(eV)
PtSe <sub>2</sub> /Sc <sub>2</sub> N	1.38%	3.02	-86.76	1.12	-0.32/1.44	-0.32/1.31
PtSe <sub>2</sub> /Sc <sub>2</sub> NF <sub>2</sub>	0.97%	2.87	-23.51	1.36	-0.02/1.38	-0.14/1.38
PtSe <sub>2</sub> /Sc <sub>2</sub> NO <sub>2</sub>	0.32%	2.55	-49.38	1.55	1.32/0.23	1.43/-0.03
PtSe <sub>2</sub> /Sc <sub>2</sub> N(OH) <sub>2</sub>	0.21%	2.03	-62.80	1.32	-0.16/1.48	-0.16/1.48

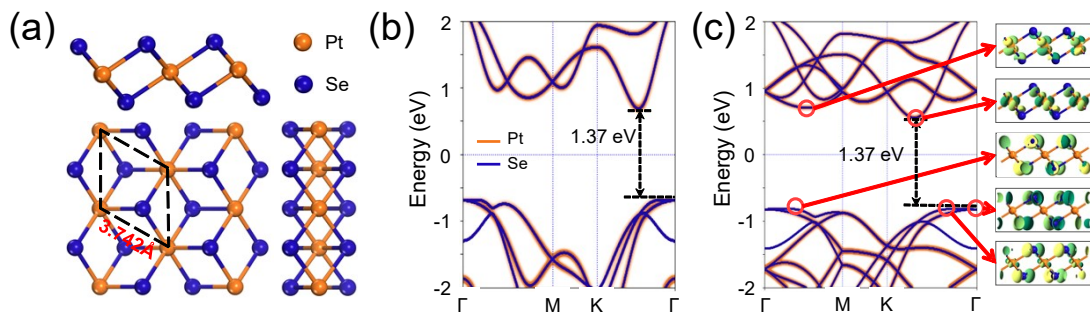


**Figure S1.** (a) The geometric structure and (b) projected band structure of ML PtSe<sub>2</sub>. (c) The projected band structure of ML PtSe<sub>2</sub> with  $\sqrt{3} \times \sqrt{3}$  supercell and Bloch states at specific k point.

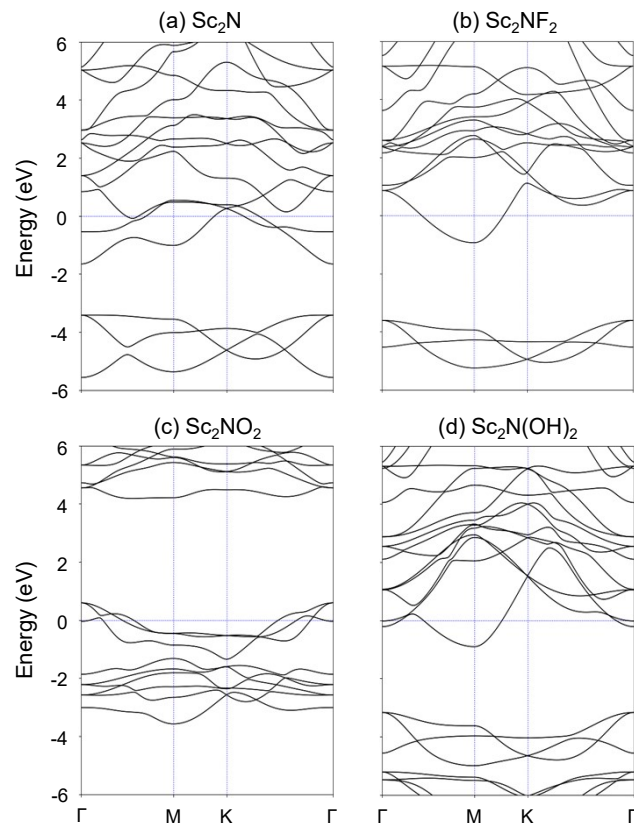


**Figure S2.** The band structures of ML Sc<sub>2</sub>N and functionalized Sc<sub>2</sub>NX<sub>2</sub> (X = F, O, and OH).

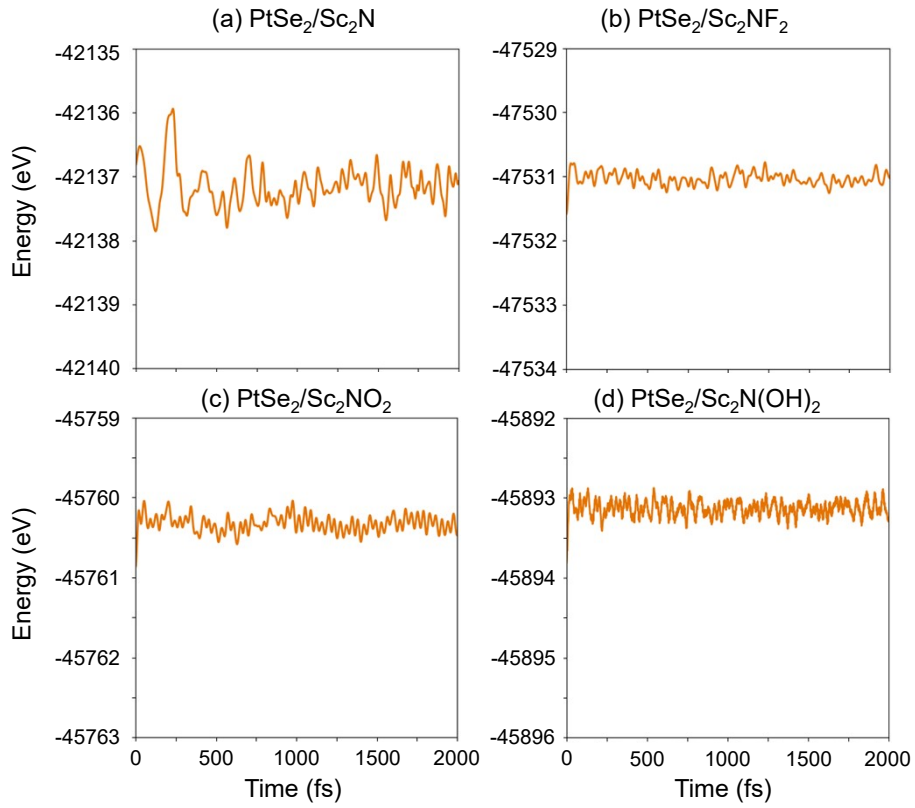


**Figure S3.** The *ab initio* molecular dynamics (AIMD) simulations of the  $\text{PtSe}_2/\text{Sc}_2\text{NX}_2$  ( $\text{X} = \text{null}, \text{F}, \text{O}, \text{and OH}$ ) vertical heterojunctions at 300 K for 2000 fs.

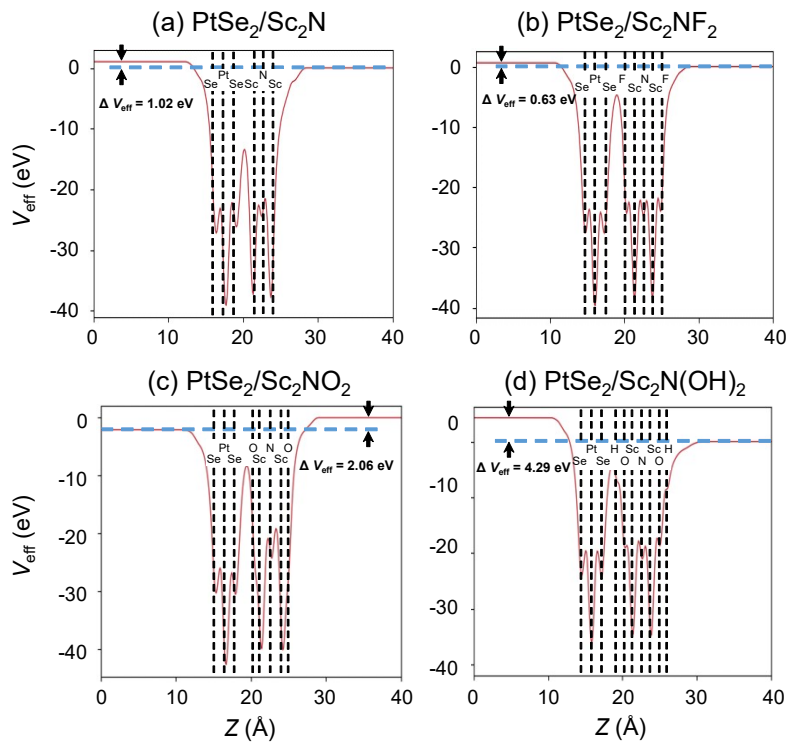
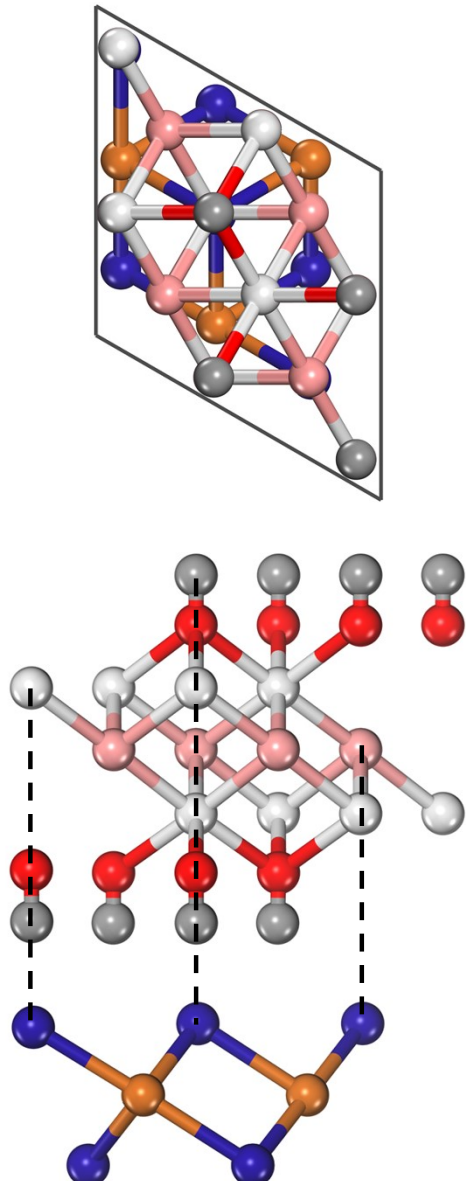


**Figure S4.** The electrostatic potentials of the  $\text{PtSe}_2/\text{Sc}_2\text{NX}_2$  ( $\text{X} = \text{null}, \text{F}, \text{O}, \text{and OH}$ ) vertical heterojunctions.

(a) stacking-Se



(b) stacking-Pt

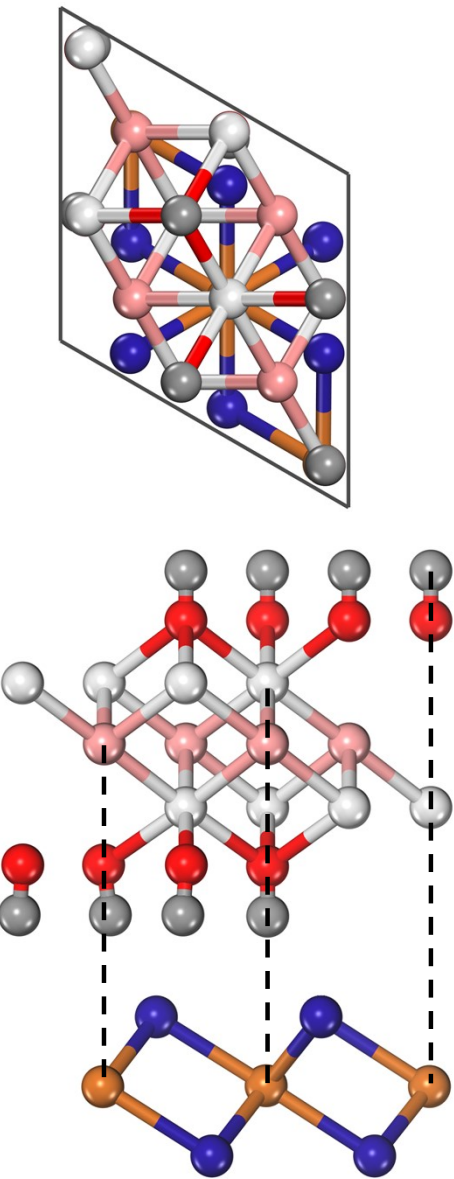


**Figure S5.** Side and top views of two more considered stacking patterns of the PtSe<sub>2</sub>/Sc<sub>2</sub>N(X)<sub>2</sub> (X=null, F, O, and OH) vertical heterojunctions with Sc<sub>2</sub>N(OH)<sub>2</sub> metal as representative.

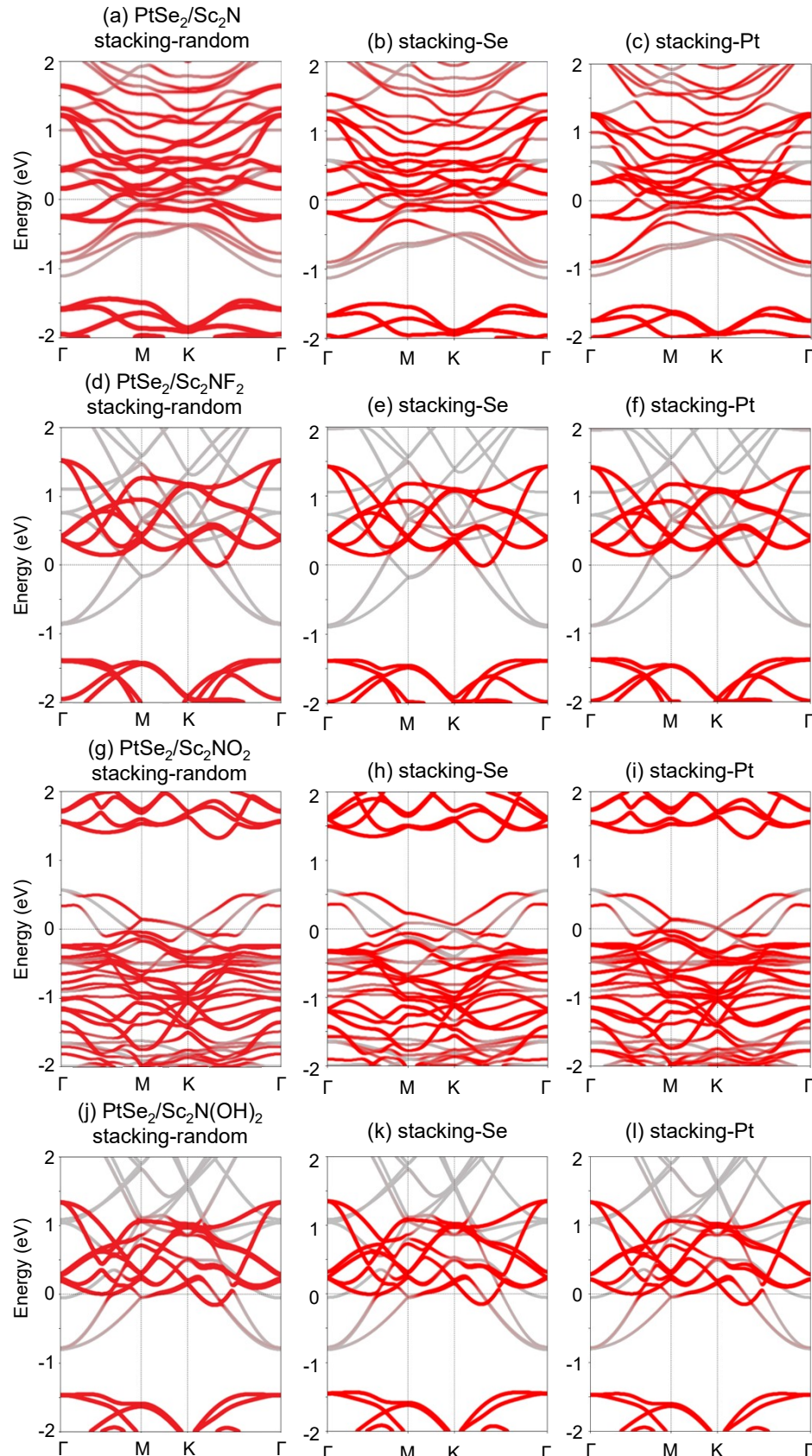


**Figure S6.** Comparison of projected band structures of the  $\text{PtSe}_2/\text{Sc}_2\text{NX}_2$  ( $\text{X} = \text{null}, \text{F}, \text{O}$ , and  $\text{OH}$ ) vertical heterojunctions with stacking patterns.

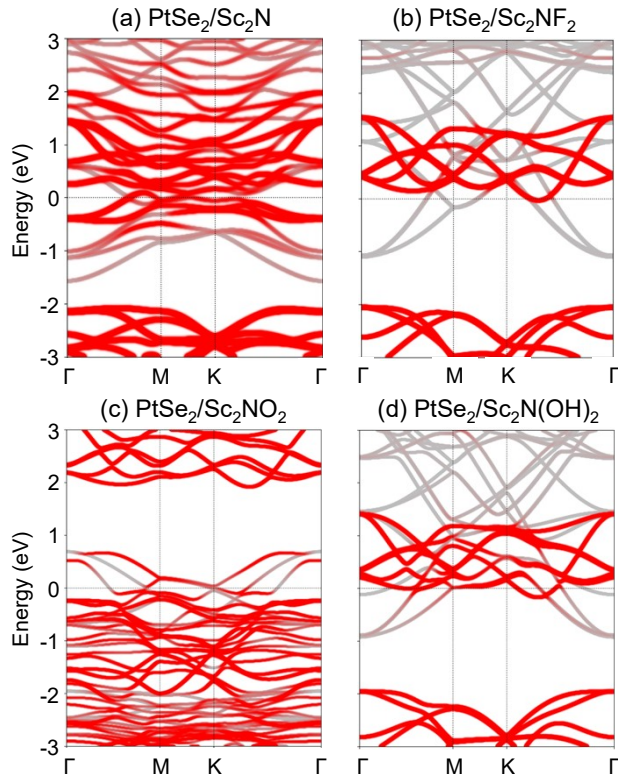


**Figure S7.** The projected band structures of the  $\text{PtSe}_2/\text{Sc}_2\text{NX}_2$  ( $\text{X} = \text{null}, \text{F}, \text{O}, \text{and OH}$ ) vertical heterojunctions at HSE06 level.